



VCU

Virginia Commonwealth University
VCU Scholars Compass

Physics Publications

Dept. of Physics

2009

Highly efficient (Cs8V) superatom-based spin-polarizer

Haiying He

Michigan Technologies Institute

Ravindra Pandey

Michigan Technologies Institute, pandey@mtu.edu

J. Ulises Reveles

Virginia Commonwealth University, jureveles@vcu.edu

Shiv N. Khanna

Virginia Commonwealth University, snkhanna@vcu.edu

Shashi P. Karna

U.S. Army Research Laboratory

Follow this and additional works at: http://scholarscompass.vcu.edu/phys_pubs



Part of the [Physics Commons](#)

He, H., Pandey, R., Reveles, J.U., et al. Highly efficient (Cs8V) superatom-based spin-polarizer. *Applied Physics Letters*, 95, 192104 (2009). Copyright © 2009 AIP Publishing LLC.

Downloaded from

http://scholarscompass.vcu.edu/phys_pubs/35

This Article is brought to you for free and open access by the Dept. of Physics at VCU Scholars Compass. It has been accepted for inclusion in Physics Publications by an authorized administrator of VCU Scholars Compass. For more information, please contact libcompass@vcu.edu.

Highly efficient (Cs_8V) superatom-based spin-polarizer

Haiying He,¹ Ravindra Pandey,^{1,a)} J. Ulises Reveles,² Shiv N. Khanna,² and Shashi P. Karna³

¹Department of Physics and Multi-Scale Technologies Institute, Michigan Technological University, Houghton, Michigan 49931, USA

²Department of Physics, Virginia Commonwealth University, Richmond, Virginia 23284-2000, USA

³Weapons and Materials Research Directorate, U.S. Army Research Laboratory, ATTN: AMSRD-ARL-WM, Aberdeen Proving Ground, Maryland 21005-5069, USA

(Received 28 August 2009; accepted 11 October 2009; published online 10 November 2009)

Quantum transport through molecules and the possibility to manipulate spin has generated tremendous excitement. Here, we demonstrate unusual spin transport through a molecule of two Cs_8V magnetic superatoms. Calculations based on density functional theory and nonequilibrium Green's function methods find a much higher current for the spin-down charge carriers relative to the spin-up carriers in the model $\text{Au}-(\text{Cs}_8\text{V})-(\text{Cs}_8\text{V})-\text{Au}$ device system with almost 100% spin polarization, indicating a highly efficient spin polarizer. The new behavior is rooted in strong coupling of the localized magnetic core on V and the itinerant electrons of the Cs shell atoms leading to nearly full spin polarization. © 2009 American Institute of Physics. [doi:10.1063/1.3259646]

The possibility of combining memory and processing in the same chip in spintronics devices has led to considerable excitement. An important step in the realization of such devices is the generation of spin polarized currents and maintaining spin coherence over long distances and times. Finding new building blocks that could allow this tantalizing prospect is currently an extremely active area of research. Systems where the electron gas could be effectively polarized and where the spin orbit interactions are fairly weak offer an attractive alternative. The purpose of this paper is to explore these options in a new class of molecules namely molecules built from superatoms.¹⁻⁶ Extensive studies over the past 25 years have shown that the electronic states of a nearly free electron gas confined by the finite cluster size are grouped into bunches of electronic shells (e.g., 1S, 1P, 1D) much in the same way as atoms (1s, 2s, 2p, 3s, 3p, 3d). These electronic shells govern the electronic, magnetic, and chemical behavior much in the same way as in atoms and this has led to the proposition that selected clusters mimicking the electronic behavior of different atoms could be regarded as superatoms forming a third dimension to the periodic table.^{4,7-9} Over the past few years, superatoms mimicking halogen, noble gases, multiple valence, alkali, and alkaline earth atoms have been proposed.⁸⁻¹⁰ In a recent paper, we extended the concept to magnetic superatoms¹¹ and proposed Cs_8V to be such a superatom.¹¹ Here, the atomic d-state electrons localized on the V site provide the spin magnetic moment while the delocalized electrons from the s-valence states of Cs and V, occupy the nearly free electron but the size-confined superatom S, P states. As each Cs atom contributes one electron, a Cs_8V cluster has a half-filled 3d atomic sub-shell localized on V, and a filled $1\text{S}^2 1\text{P}^6$ superatom shells stabilizing the cluster, and thus leading to a magnetic superatom. Our earlier studies suggested that a superatom dimer complex, $(\text{Cs}_8\text{V}-\text{Cs}_8\text{V})$ composed of magnetic

superatoms has competing ferromagnetic and antiferromagnetic configurations.¹¹ The combination of alkali atoms and V has the added advantage of weak spin-orbit interaction reducing spin decoherence due to such a coupling. Here we demonstrate that the magnetic superatoms can lead to unusual molecular electronic properties including a highly efficient spin polarization at room temperature—offering themselves a new class of material for realizable spin nano-electronics.

The quantum transport of electrons via a model system consisting of the superatom $(\text{Cs}_8\text{V})-(\text{Cs}_8\text{V})$ complex sandwiched between two Au contacts (Fig. 1) was investigated employing state-of-the-art density functional theory together with the nonequilibrium Green's function (NEGF) method. The central scattering region includes eight 6×6 $\text{R}(001)$ Au layers on either side of the electrodes. In order to eliminate the interfacial effects, Au atoms are directly bonded to the superatoms. The separation between the superatom and the electrodes was 3.5 \AA which is close to the calculated Cs-Au distance of 3.23 \AA in a diatomic molecule. *First principles* electronic structure calculations were performed within the local spin density approximation of the exchange and correlation functional,^{12,13} incorporated in the SIESTA¹⁴ software. The bias-dependent electron transmission and current due to individual spin, I^\uparrow and I^\downarrow , are then calculated from the NEGF method integrated with SIESTA, as implemented in the *ab initio* transport code SMEAGOL.^{15,16} Norm-conserving pseudopotentials¹⁷ and double-zeta basis sets with polariza-

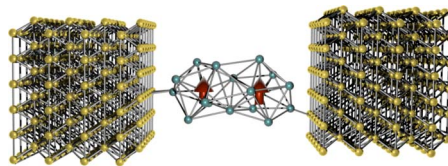


FIG. 1. (Color online) A schematic illustration of a superatom-based model system: $\text{Au}-(\text{Cs}_8\text{V})-(\text{Cs}_8\text{V})-\text{Au}$. Large, medium, and small balls represent Au, Cs, and V atoms respectively. The arrows indicate the direction of the V local spin moments in a ferromagnetic configuration.

^{a)}Author to whom correspondence should be addressed. Electronic mail: pandey@mtu.edu.

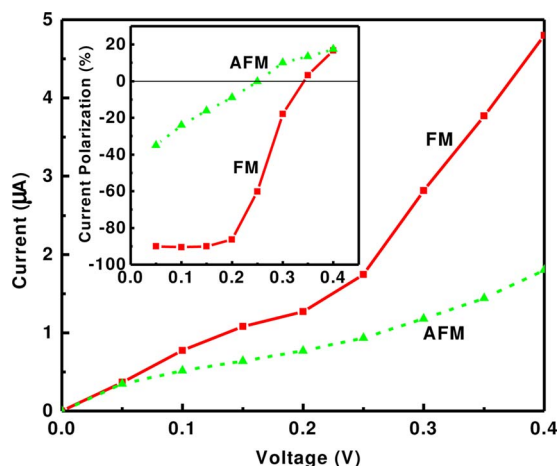


FIG. 2. (Color online) Current-voltage characteristic of the model system where current polarization $[P=(I^\uparrow - I^\downarrow)/(I^\uparrow + I^\downarrow)]$ as a function of applied bias voltage is shown in the inset. FM and AFM represent ferromagnetic and antiferromagnetic spin configurations, respectively.

tion orbitals were used on Cs and V atoms; while a single-zeta basis set was used for Au with only 6s as the valence electron.¹⁸ The charge density is obtained by integrating the Green's function over 200 imaginary and 1000 real energy points giving rise to less than 0.03% deviation in the total charge of the system. More details of the theoretical method are given in the supporting information.¹⁸

First principles calculations predict the antiferromagnetic and ferromagnetic isomers of the $(\text{Cs}_8\text{V})-(\text{Cs}_8\text{V})$ superatom complex to be nearly degenerate; the antiferromagnetic case being lower in energy by 0.06 eV. The (average) bond lengths of Cs–Cs and Cs–V in the complex are calculated to be 5.01 and 4.26 Å, respectively. The ferromagnetic isomer of the complex has a magnetic moment of $12\mu_B$, which is only 0.03 eV lower than the state with a magnetic moment of $10\mu_B$. The higher magnetic moment in the former is mainly due to the induced spin polarization over Cs atoms. We note here that the ground state of the (Cs_8V) monomer “superatom” has a nonzero magnetic moment of $5\mu_B$.¹¹

The calculated current-voltage (I - V) characteristics of the $(\text{Cs}_8\text{V})-(\text{Cs}_8\text{V})$ superatom complex are shown in Fig. 2. The calculations predict a large magnetoresistive effect in the complex above 50 mV with the current in the ferromagnetic state being significantly higher than that in the antiferromagnetic state. Note that the applied voltage ranges from 0 to 400 mV corresponding to maximum electric field strength of 1.86×10^8 V/m, assuming a uniform electric field is applied between the Au electrodes. The antiferromagnetic state shows ohmic (linear) I - V characteristics in the bias region of 0–400 mV. In contrast, the I - V characteristics of the ferromagnetic state show an interesting, but unusual feature in the high bias region (>250 mV)—the rate of the increase in the tunneling current is much higher than that in the low bias region (<250 mV).

The bias (voltage)-dependence of conductance (current) of the model device can be understood from an analysis of the transmission function, which, in general, reflects the intrinsic transport characteristics of the system. We note that the tunneling current is obtained by integrating the transmission function within the bias voltage window. The transmission functions, shown in Fig. 3, suggest the superatom system to be metallic in both ferromagnetic and antiferro-

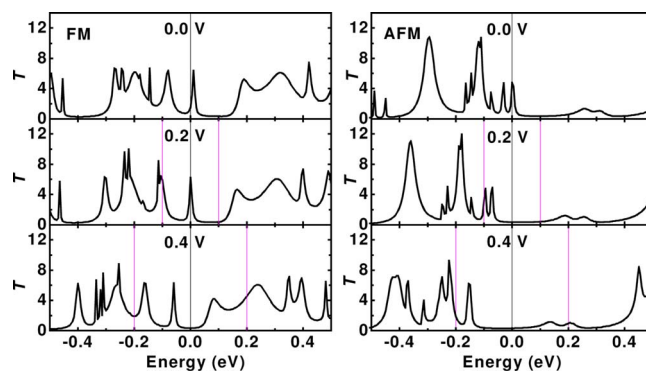


FIG. 3. (Color online) Transmission function (T) of the model device. The zero of the energy is aligned to the Fermi energy and the bias window is indicated by gray lines. FM and AFM represent, respectively, ferromagnetic and antiferromagnetic spin configurations of the system.

magnetic spin configurations with a finite number of scattering states at the Fermi energy (E_F). It is consistent with the fact that the monomer (Cs_8V) superatom has delocalized electrons in its outer shell which give it the characteristics of metallic atom.¹¹ An analysis of these scattering states via projected density of states further confirms their character to be associated with Cs atoms, whereas the states mostly associated with V atoms form narrow peaks about 100–200 meV below E_F (see for example Fig. 4). These V states forming the core of the superatom result in resonance electron transmission. As the bias increases from zero to 200 and then to 400 mV, there appears to be an increase in the number of states in the bias voltage window which, in turn, contributes to the increase in the tunneling current across the system (Fig. 3).

It is interesting to note the strong spin-polarization of current in the ferromagnetic state of the superatom complex, which is absent or negligible in the antiferromagnetic state. This feature is reflected in the inset of Fig. 2 showing the bias voltage dependence of the current polarization (P) which is defined as $[P=(I^\uparrow - I^\downarrow)/(I^\uparrow + I^\downarrow)]$. For the low bias region (<250 mV), the results find the polarization to be negative (i.e., $I^\downarrow \gg I^\uparrow$) suggesting the majority carriers to be associated only with the spin-down electrons in the model

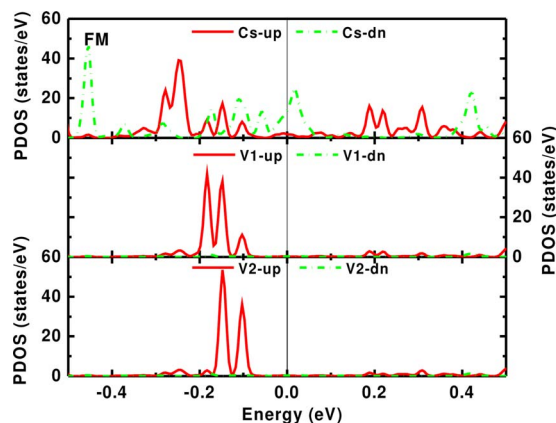


FIG. 4. (Color online) Projected Density of States of the ferromagnetic spin configuration of the model system. Zero of the energy is aligned to the Fermi energy. The contributions from both spin-up (up) and spin-down (dn) electrons are plotted from the top to the bottom panel for Cs (a summation of all the Cs atoms), the first V (V1) and the second V (V2) atoms, respectively.

system. As the bias voltage increases, contributions from the spin-up electrons become equal to that of the spin-down electrons leading to negligible current polarization at 350 mV. This unique feature of the model system based on the (Cs₈V) superatoms can be tremendously beneficial in spin nanoelectronics as efficient spin-polarizer. In the low bias voltage regime, the proposed system is predicted to be efficient

with nearly 100% polarization (inset of Fig. 2) and could be used to realize room-temperature operational spin nanoelectronics devices. This nearly-full spin polarization is competitive to that of the newly-developed half-metals [such as La_{0.66}Sr_{0.33}MnO₃ P=96% (Ref. 19) and CrO₂ P=98% (Ref. 20)] and significantly higher than the traditional ferromagnetic transition metals [such as Fe, Co, and Ni P=40–50% (Refs. 21–23)].

Since there is a general correspondence between the transmission function and the density of states of the system, a deeper insight can be gained via a close examination of the projected density of states for both the spin-up and the spin-down electrons. The antiferromagnetic state (not shown here) has a well-balanced distribution of the density of states for the spin-up and the spin-down electrons. In contrast, the relative shift in the spin-up and spin-down components are distinct in the ferromagnetic state as shown in Fig. 4. There appears a strong hybridization of the V d-states with the Cs s-states in the energy of about 200 meV below E_F , which induces the exchange split of the spin-up and spin-down electrons in the Cs s-shells. This leads to a major contribution of density of states from the spin-down electrons of Cs atoms in the close proximity of E_F , while the spin-up component becomes negligible near E_F .

Ferromagnetic transition metals suffer from the low polarization for high itinerant sp-type electrons. In the present case, we have shown that coupling the electrons of the magnetic core atom and the itinerant electrons of the shell atoms can considerably enhance the spin-polarization of the shell conducting electrons to its full limit. It is also worth noting that in the proposed architecture it is also possible to enlarge the energy range for high spin-polarization via gating. For example, in the ferromagnetic state of the model architecture, shifting the bias window to 200–400 meV above E_F , significantly increases the current due to the spin-up electrons over spin-down electrons and can lead to even higher positive spin polarization (see Fig. 4)

The present work demonstrates that “magnetic superatom” assemblies can lead to unusual spin transport and can find applications in a wide-variety of spin-dependent electronics devices. One can envision spin transport in a linear chain of such superatoms. Since the s-electrons in the Cs

atoms have no spin-orbit coupling, such a system will maintain spin coherence over a long travel distance and time. The large, nearly 100% spin polarization calculated in the Cs₈V–Cs₈V magnetic superatom offers a new mechanism and architecture for realizing highly efficient spin-polarizers for applications in spin nanoelectronics.

Helpful discussions with S. Gowtham are acknowledged. The work at Virginia Commonwealth University was supported by the U. S. Department of the Army through a MURI Grant No. W911NF-06-1-0280.

¹W. A. de Heer, W. D. Knight, M. Y. Chou, and M. L. Cohen, *Solid State Phys.* **40**, 93 (1987).

²S. N. Khanna and P. Jena, *Phys. Rev. B* **51**, 13705 (1995).

³E. Janssens, S. Neukermans, and P. Lievens, *Curr. Opin. Solid State Mater. Sci.* **8**, 185 (2004).

⁴D. E. Bergeron, A. W. Castleman, Jr., T. Morisato, and S. N. Khanna, *Science* **304**, 84 (2004).

⁵J. Hartig, A. Stösser, P. Hauser, and H. A. Schnöckel, *Angew. Chem., Int. Ed.* **46**, 1658 (2007).

⁶M. Walter, J. Akola, O. Lopez-Acevedo, P. D. Jadzinsky, G. Calero, C. J. Ackerson, R. L. Whetten, H. Groenbeck, and H. Hakkinen, *Proc. Natl. Acad. Sci. U.S.A.* **105**, 9157 (2008).

⁷A. W. Castleman, Jr. and S. N. Khanna, *J. Phys. Chem. C* **113**, 2664 (2009).

⁸D. E. Bergeron, P. J. Roach, A. W. Castleman, Jr., N. O. Jones, and S. N. Khanna, *Science* **307**, 231 (2005).

⁹J. U. Reveles, S. N. Khanna, P. J. Roach, and A. W. Castleman, Jr., *Proc. Natl. Acad. Sci. U.S.A.* **103**, 18405 (2006).

¹⁰A. W. Castleman, Jr., S. N. Khanna, A. Sen, A. C. Reber, M. Qian, K. M. Davis, S. J. Peppernick, A. Ugrinov, and M. D. Merritt, *Nano Lett.* **7**, 2734 (2007).

¹¹J. U. Reveles, P. A. Clayborne, A. C. Reber, S. N. Khanna, K. Pradhan, P. Sen, and M. R. Pederson, *Nat. Chem.* **1**, 310 (2009).

¹²D. M. Ceperley and B. J. Alder, *Phys. Rev. Lett.* **45**, 566 (1980).

¹³J. P. Perdew and A. Zunger, *Phys. Rev. B* **23**, 5048 (1981).

¹⁴J. M. Soler, E. Artacho, J. D. Gale, A. Garcia, J. Junquera, P. Ordejon, and D. Sanchez-Portal, *J. Phys.: Condens. Matter* **14**, 2745 (2002).

¹⁵A. R. Rocha, V. M. García Suárez, S. W. Bailey, C. J. Lambert, J. Ferrer, and S. Sanvito, *Nature Mater.* **4**, 335 (2005).

¹⁶A. R. Rocha, V. M. Garcia-Suarez, S. Bailey, C. Lambert, J. Ferrer, and S. Sanvito, *Phys. Rev. B* **73**, 085414 (2006).

¹⁷N. Troullier and J. L. Martins, *Phys. Rev. B* **43**, 1993 (1991).

¹⁸See EPAPS supplementary material at <http://dx.doi.org/10.1063/1.3259646> for details of the theoretical method.

¹⁹B. Nadgorny, I. I. Mazin, M. Osofsky, R. J. Soulen, P. Broussard, R. M. Stroud, D. J. Singh, V. G. Harris, A. Arsenov, and Y. Mukovskii, *Phys. Rev. B* **63**, 184433 (2001).

²⁰A. Anguelouch, A. Gupta, G. Xiao, D. W. Abraham, Y. Ji, S. Ingvarsson, and C. L. Chien, *Phys. Rev. B* **64**, 180408 (2001).

²¹R. J. Soulen, Jr., J. M. Byers, M. S. Osofsky, B. Nadgorny, T. Ambrose, S. F. Cheng, P. R. Broussard, C. T. Tanaka, J. Nowak, J. S. Moodera, A. Barry, and J. M. D. Coey, *Science* **282**, 85 (1998).

²²T. H. Kim and J. S. Moodera, *Phys. Rev. B* **69**, 020403 (2004).

²³M. Cinchetti, M. S. Albanda, D. Hoffmann, T. Roth, J.-P. Wuestenberg, M. Krauss, O. Andreyev, H. C. Schneider, M. Bauer, and M. Aeschliemann, *Phys. Rev. Lett.* **97**, 177201 (2006).